b-production at the Tevatron

Eric Kajfasz

b-production at the Tevatron

Eric Kajfasz for the CDF and DØ collaborations
Fermilab, P.O. Box 500, Batavia, IL 60510, USA
CPPM, Case 907, Faculté des Sciences de Luminy, 13288 Marseille Cedex 9, France

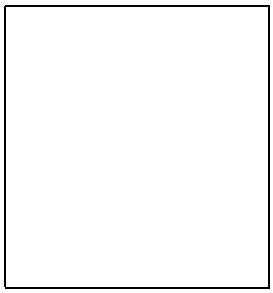

The phenomenology of b-production and some of the previous Run I measurements of CDF and DØ are briefly reviewed. A new analysis by CDF of Run I $b\bar{b}$ angular correlations and a new measurement by DØ of Run II b-jet cross-section, are presented.

1 Introduction

The measurement of b quark production in high energy hadronic collisions provides an essential test bench for how well we understand QCD, especially in its perturbative regime. Indeed, the b quark is heavy enough ($m_b \gg \Lambda_{QCD}$) to justify perturbative expansions, however, it is still light enough to be produced copiously at the Tevatron.
After summarizing some of CDF and DØ Run I results, we present the new preliminary results on B-hadron correlations that CDF recently extracted from its Run I data, and a preliminary DØ b-jet cross-section coming from an analysis of Run II data collected with the upgraded DØ detector.

2 Some of previous CDF and DØ Run I results

Theoretical spectra at Next to Leading Order (NLO) have been available for some time [1], but they show a discrepancy by up to a factor 2 to 4 with respect to experimental spectra measured by CDF [2] and DØ [3] in Run I at the Tevatron.
Fig. 1 shows a compilation of CDF and DØ measurements of the integrated b-quark cross-section as a function of the minimum transverse momentum of the b, P_T^{min}, in the central rapidity region $|y^b| < 1$. The measurements are compared to the NLO QCD prediction shown as a dashed line. As a general trend, this discrepancy seems to be less accute at higher P_T^{min}. DØ also showed [3] (see fig. 2) that this discrepancy worsens at higher rapidities.

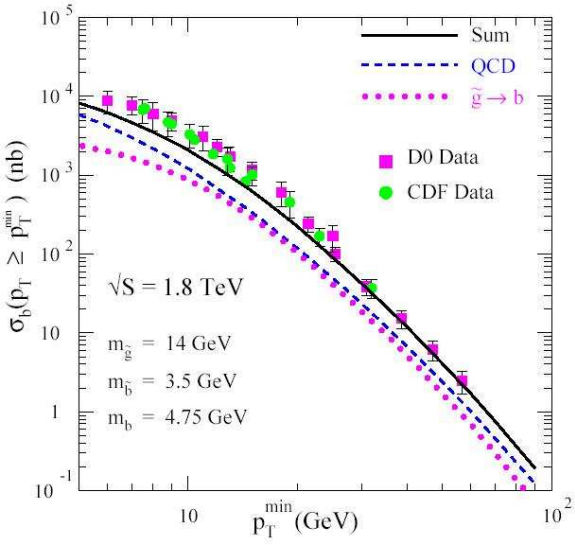

Figure 1: CDF and D0 Run I data compared to NLO QCD predictions and to the model discussed in [5].

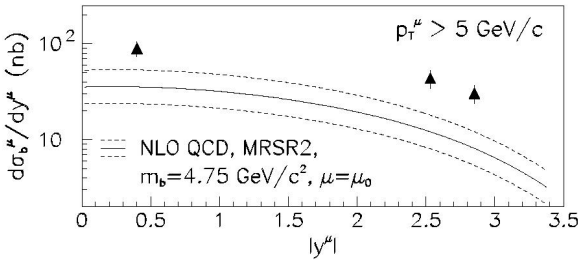

Figure 2: D0 Run I measurement of b production in the forward region compared to NLO QCD predictions.

P_T distributions for open b-quark production are sensitive to large log terms, which need to be resummed to all orders, and to non-perturbative corrections required to account for the fact that hadrons, not quarks, are the measured final states. To prevent such a sensitivity, it has been suggested [4] that one could look at E_T distributions of b-jets, instead. Fig. 3 shows the measurement performed by D0 in run I compared to the NLO QCD calculations [4]. The better agreement between theory and measurement seen here may hint at some possible improvement to be made e.g. in the heavy quark fragmentation functions.

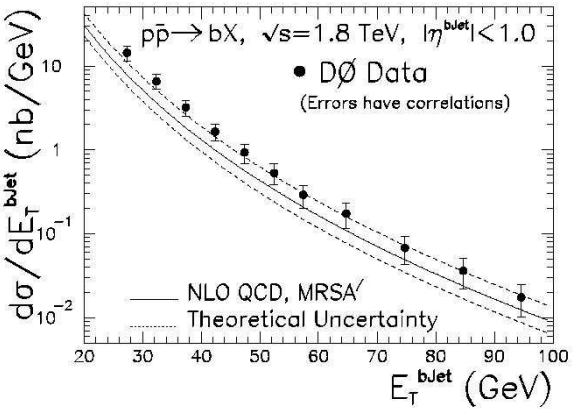

Figure 3: D0 Run I B-hadron production cross-section compared to NLO QCD predictions.

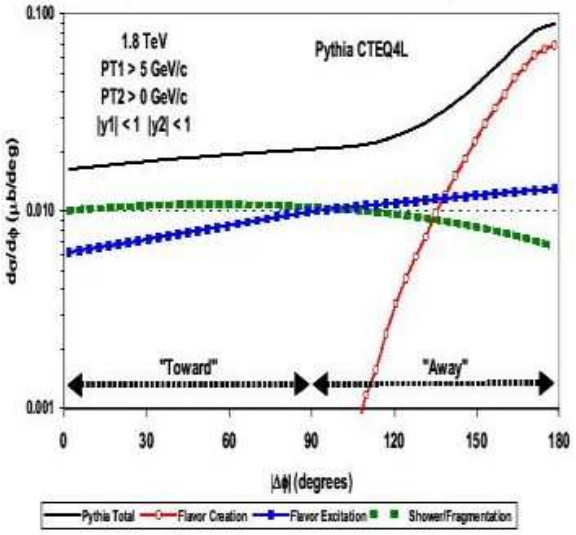

Figure 4: Predicted PYTHIA angular correlations for the 3 sources of beauty (from [6]). $\Delta\phi$ is the azimuthal angle between b and $\bar{b}$.

The work done to try to better understand the situation mainly goes into three directions:
Sources of b-quarks: at leading order, b-quarks are produced through $q\bar{q}$ annihilations and gg fusion. But, at higher orders, two other mechanisms come into play, namely, flavor excitation and gluon splitting [6]. The amount with which these different production mechanisms contribute at the Tevatron depends on a number of theoretical uncertainties. From an experimental point

of view, as shown in Fig. 4, the $b\bar{b}$ azimuthal opening angle $\Delta\phi$ for the three sources are quite different and can be used to attempt to isolate their individual contributions [6]. Flavor creation tends to produce b and $\bar{b}$ mostly back to back. Its $\Delta\phi$ distribution does not show any contribution in the "Towards" region ($\Delta\phi < 90°$). This will be elaborated on in section 3.
Resummations and Fragmentation Functions:
It has been shown [8] that NLO QCD with $\overline{\text{MS}}$ renormalization scheme, together with non-perturbative fragmentation functions extracted from LEP and SLC data, can give a good agreement with CDF Run I B meson cross-section measurement.
Using a Fixed Order plus Next to Leading Log (FONLL) b quark spectrum and fitting the moments rather than the shape of the non-perturbative fragmentation function from $e+e-$ data, has also proven [7] to provide a better agreement with CDF and D0 Run I measurements, as can be seen in Fig. 5.
New physics: an interesting possibility has been explored in [5]. The dotted line on Fig. 1 shows how the production ($p\bar{p} \to \tilde{g}\tilde{g}$) of relatively light gluinos followed by their decay into b and and a light $\tilde{b}$ could help reduce the discrepancy.

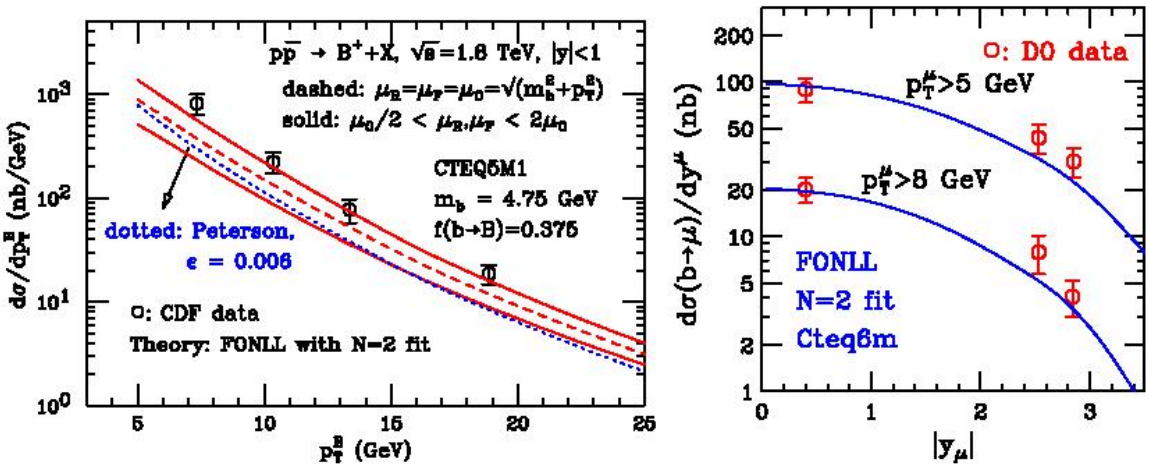

Figure 5: Run I data using tweaked resummation and fragmentation functions as discussed in [7].

3 New CDF $b\bar{b}$ angular correlations from Run I data

In this analysis, CDF uses 90 pb^{-1} of a data sample taken during the run IB of the Tevatron (1994-1995) with collisions at a center of mass energy of 1.8 TeV. A muon or an electron trigger is required in order to enrich the b content of the data analyzed. Tracking information is used to reconstruct the decay vertices of both B hadrons. Decay vertices angular correlations are then compared to PYTHIA predictions.

3.1 secondary vertex correlations

Figure 6 shows, for the data with an electron trigger, the opening angle $\Delta\phi$ between the momentum vectors of the secondary vertices in the transverse plane. Detector effects are simulated in Monte Carlo. The relative contribution from flavor creation, flavor excitation, and gluon splitting are varied to give a best match to the data. Similar distributions are also produced for data with a muon trigger.

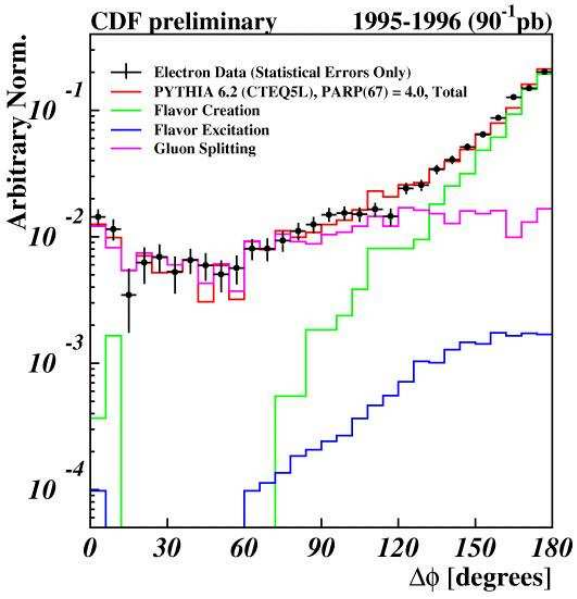

Figure 6: Measured secondary vertex correlations compared to PYTHIA with relative contributions of the different sources adjusted to give best match.

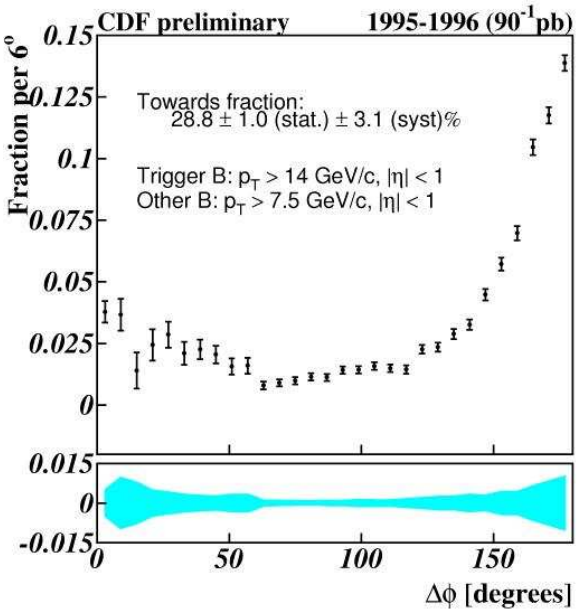

Figure 7: Measured B-hadron correlations.

3.2 measured B-hadron correlations

Figure 7 shows, for a total of 17,000 e+μ events, the opening angle $\Delta\phi$ between the measured B directions in the transverse plane. The detector effects are unfolded from data using PYTHIA. Also taken into account are corrections for mistags, tags from prompt charm, and sequential double tags. The fraction of events in the "Towards" region ($\Delta\phi < 90°$), where flavor excitation and gluon splitting contribute, is measured to be $28.8 \pm 1.0(stat) \pm 3.1(syst)\%$. The shaded region shows the correlated systematic errors. The error bars show statistical errors only.

4 DØ Run II *b*-jet cross-section

This analysis utilizes 3.4 pb^{-1} of data, collected with the upgraded DØ detector between end of February and mid-May 2002 as part of the Run II of the Tevatron, with collisions at a center of mass energy of 1.96 TeV.

4.1 μ+jet cross-section

First, the cross-section for the muons associated with jets is measured. Jets are defined with a $R = \sqrt{\Delta\eta^2 + \Delta\phi^2} = 0.5$ cone algorithm. The muon track is measured by the muon system only and the kinematic cuts used are:
$|\eta^{jet}| < 0.6$, $|E_T^{jet}| > 20$ GeV, $|\eta^{\mu}| < 0.8$, $P_T^{\mu} > 6$ GeV, $|\Delta R(jet, \mu)| < 0.7$
The jet reconstruction efficiency is 100% for $E^{jet} > 20$ GeV, the muon reconstruction efficiency is $43.7 \pm 0.8(stat) \pm 2.2(syst)\%$.

4.2 b-tagging and b-jet fraction

Then, the b content of the sample is estimated by identifying the jets emanating from b quarks. In this analysis, the tagging of b-jets is done by calculating the P_T^{rel} for the muons associated with jets (see P_T^{rel} definition in Fig. 8). The method is based on the fact that, because of the

high mass of the b quark, the muons produced in the decay of the b-quark have a higher P_T^{rel} than the muons produced in other processes.

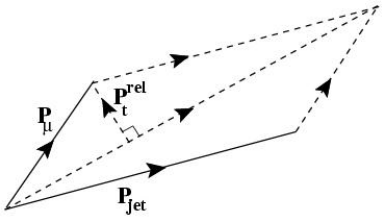

Figure 8: Definition of P_T^{rel}

Since the shape of the P_T^{rel} distribution depends on the energy of the jet, the E_T^{jet} range is divided into several bins. In each of these bins, the P_T^{rel} distribution for the data is adjusted to the sum of a signal template (extracted from a $b \rightarrow \mu$ Monte Carlo simulation) and of a background template (extracted from 1.5 million QCD events). Because of the satistical limitations of the background templates, four E_T^{jet} bins are used. The resulting b-jet fraction as a function of E_T^{jet} is given in Fig. 9, including a functional form $a + b/E_T^{jet}$ fitted to the measurements.

4.3 b-jet cross-section

The b-jet cross-section is obtained by folding the μ+jet cross-section with the b-jet fraction and by unfolding it from the calorimeter jet energy resolution using an ansatz function. The preliminary Run II result is shown in Fig. 10 compared to theoretical predictions (solid line). The band within the dashed lines covers the theoretical uncertainties. This measurement is consistent with the corresponding Run I result shown in section 2.

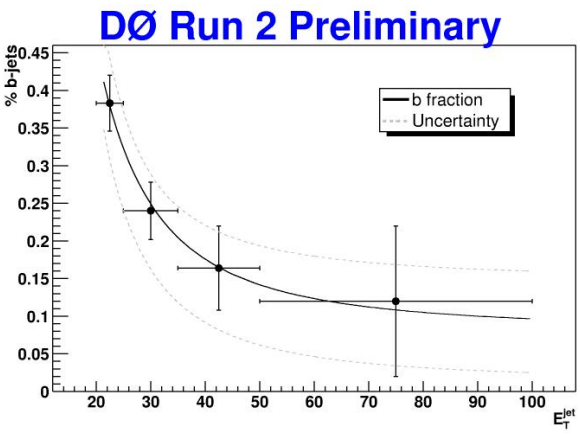

Figure 9: b-jet fraction as a function of E_T^{jet}.

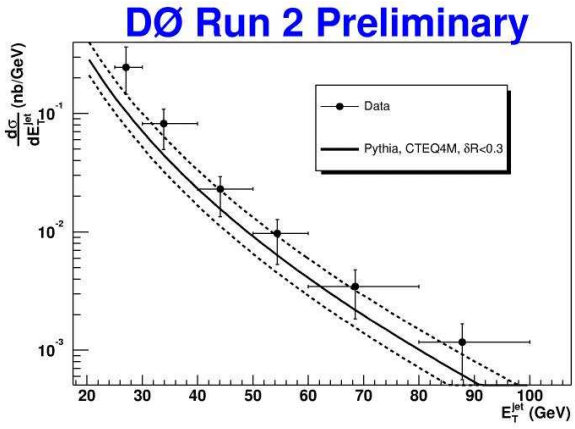

Figure 10: Measured Run II b-jet cross section compared to theoretical predictions.

5 Conclusions

Although the agreement between calculated and measured b-production spectra is still not perfect, our understanding is steadily progressing, both on the theoretical and experimental sides. There is still room left for improvement and maybe new physics. New Run II data at the Tevatron from both CDF and DØ will hopefully help to shed light on the remaining obscure corners of this long standing issue, soon.

References

1. P. Nason, S. Dawson, and R. K. Ellis *Nucl. Phys.* B303, 607 (1988); *Nucl. Phys.* B327, 49 (1989);*Nucl. Phys.* B335, 260 (1990)
   W. Beenaker *et al. Phys. Rev.* D40, 54 (1993); *Nucl. Phys.* B351, 507 (1991)
2. F. Abe *et al. Phys. Rev.* D50, 4252 (1994); *Phys. Rev. Lett.* 75, 1451 (1995); *Phys. Rev.* D53, 1051 (1996)
   D. Acosta *et al. Phys. Rev.* D65, 052005 (2002)
3. S. Abachi *et al. Phys. Rev. Lett.* 74, 3548 (1995)
   B. Abbott *et al. Phys. Lett.* B487, 264 (2000); *Phys. Rev. Lett.* 84, 5478 (2000); *Phys. Rev. Lett.* 85, 5068 (2000)
4. S. Frixione et M. L. Mangano *Nucl. Phys.* B483, 321 (1997)
5. E. L. Berger *et al. Phys. Rev. Lett.* 86, 4231 (2001)
6. R. D. Field *Phys. Rev.* D65, 094006 (2002) and hep-ph/0201112
7. M. Cacciari, P. Nason *Phys. Rev. Lett.* 89, 122003-1 (2002)
   P. Nason *Heavy Flavor Production* hep-ph/0301003
8. J. Binnewies *et al. Phys. Rev.* D58, 030416 (1998)
   B. A. Kniehl hep-ph/0211008